JOURNAL OF THERMOPHYSICS AND HEAT TRANSFER
Vol. 18, No. 2, April–June 2004

Thermal Contact Resistance of Nonconforming Rough Surfaces, Part 1: Contact Mechanics Model

M. Bahrami,* J. R. Culham,† M. M. Yovanovich,‡ and G. E. Schneider§
University of Waterloo, Waterloo, Ontario N2L 3G1, Canada

A new analytical model for spherical rough contacts, in the form of a set of relationships, is developed and solved numerically. It is shown that the maximum contact pressure is the parameter that specifies the contact pressure distribution. Simple correlations for calculating the maximum contact pressure and the radius of the macrocontact area as functions of the nondimensional parameters are proposed. A relationship for pressure distributions is derived where the load is higher than the critical load. A general pressure distribution is developed that covers the entire range of spherical contacts from the smooth Hertzian to the conforming rough contact. Finally, a criterion is derived to identify flat surfaces where the surface curvature has negligible effect on the contact pressure.

Nomenclature

A	=	area, m^2
a	=	radius of contact, m
a'_L	=	relative radius of macrocontact, a_L/a_H
a_s	=	radius of microcontacts, m
b	=	flux tube radius, m
c_0	=	function of τ, $1.8\ \tau^{-0.028}$
c'_0	=	function of τ, $0.31\ \tau^{0.056}$
c_1	=	Vickers microhardness coefficient, GPa
c_2	=	Vickers microhardness coefficient
dr	=	increment in radial direction, m
d_v	=	Vickers indentation diagonal, μm
E	=	Young's modulus, GPa
E'	=	equivalent elastic modulus, GPa
F	=	external force, N
F^*	=	relative force error
f_i	=	discrete point forces, N
H_{mic}	=	microhardness, GPa
m	=	mean absolute surface slope
n_s	=	number of microcontacts
P	=	pressure, Pa
P'_0	=	relative maximum pressure, $P_0/P_{0,H}$
r, z	=	cylindrical coordinates
u	=	sphere profile, m
u_0	=	maximum indentation, m
Y	=	mean surface plane separation, m
α	=	nondimensional parameter, $\sigma\rho/a_H^2$
β	=	summits radii of curvature, m
γ	=	general pressure distribution exponent
δ	=	max surface out-of-flatness, m
η_s	=	microcontacts density, m^{-2}
λ	=	nondimensional separation, $Y/\sqrt{(2)}\sigma$
ν	=	Poisson's ratio
ξ	=	nondimensional radial position, r/a_L
ρ	=	radius of curvature, m
σ	=	rms surface roughness, μm
τ	=	nondimensional parameter, ρ/a_H
ω_b	=	bulk normal deformation, m

Subscripts

a	=	apparent
b	=	bulk
c	=	critical
H	=	Hertz
L	=	large, macro
r	=	real
s	=	small, summit
v	=	Vickers
0	=	value at origin
1, 2	=	surface 1, 2

Received 26 May 2003; presented as Paper 2003-4197 at the AIAA 36th Thermophysics Conference Meeting, Orlando, FL, 23–26 June 2003; revision received 12 August 2003; accepted for publication 13 August 2003.

*Ph.D. Candidate, Department of Mechanical Engineering; majid@mhtlab.uwaterloo.ca.
†Associate Professor, Director, Microelectronics Heat Transfer Laboratory.
‡Distinguished Professor Emeritus, Department of Mechanical Engineering. Fellow AIAA.
§Professor, Department of Mechanical Engineering. Associate Fellow AIAA.

Introduction

An accurate knowledge of contact mechanics, that is, the pressure distribution, the size of contact area, and the mean separation between surface planes as functions of applied load, and the geometrical and mechanical characteristics/properties of the contacting bodies, plays an important role in predicting and analyzing thermal and electrical contact resistance and many tribological phenomena.

The contact of two spherical rough surfaces includes two problems with different scales, 1) the bulk- or macroscale problem, that is, bulk elastic compression, which can be calculated using the Hertz[1] theory for ideal smooth mean profiles of two surfaces, and 2) the small- or microscale problem, that is, deformation of surface asperities. The scales of the subproblems (macro and micro) are very different yet, at the same time, strongly interconnected. Because of surface roughness, contact between two surfaces occurs only at discrete microscopic contacts and the real area of contact, the total area of these microcontacts, is typically a small fraction of the nominal contact area.[2,3] The macrocontact area is defined as the area in which the microcontacts are distributed, also the contact pressure falls off to a negligible value at the edge of the macrocontact. The surface asperities act like a compliant layer on the surface of the contacting bodies, so that the contact is extended over a larger apparent area than it would be if the surfaces were smooth, and consequently, the contact pressure for a given load will be reduced.[4]

Developing an analytical model, which enables one to predict the contact parameters such as pressure distribution and the size of the macrocontact area, is the main goal of this study. It is also required to find simple correlations for determining the contact parameters that can be used in analytical thermal contact models. Another purpose

of this research is to find a criterion to define the flat surface where the surface curvature can be neglected.

Theoretical Background

As already mentioned, the spherical rough contact mechanics problem is divided into macro- and micro-sub-problems. The macro-problem is the contact of two spherical bodies, which in this study is assumed to be within the elastic limit, and the micro or the deformation of the surface asperities is assumed to be plastic.

Microcontact Modeling

The solution of any contact mechanics problem requires that the geometry of the intersection and overlap of the two undeformed surfaces be known as a function of their relative position. If the asperities of a surface are isotropic and randomly distributed over the surface, the surface is called Gaussian. Williamson et al.[5] have shown experimentally that many of the techniques used to produce engineering surfaces give a Gaussian distribution of surface heights. Many researchers, including Greenwood and Williamson[3] assumed that the contact between two Gaussian rough surfaces can be simplified to the contact between a single Gaussian surface, having the effective (sum) surface characteristics, placed in contact with a perfectly smooth surface, as shown in Fig. 1. The equivalent roughness σ and surface slope m can be found from

$$\sigma = \sqrt{\sigma_1^2 + \sigma_2^2}, \qquad m = \sqrt{m_1^2 + m_2^2} \tag{1}$$

Bahrami et al.,[6] based on the deformation mode of asperities, categorized existing microcontact mechanical models into three main groups: elastic, plastic, and elastoplastic. By comparing the elastic model of Greenwood and Williamson[3] and the plastic model of Cooper et al.[7] for nominal flat contacts, Bahrami et al.[6] showed that the behavior of the preceding models are similar, despite the different assumed deformation mode of asperities. They also concluded that, in most real contacts, asperities deform plastically except for special cases where the surfaces are extremely smooth; see Bahrami et al.[6] for more detail.

The present model is developed assuming the asperities deform plastically. Plastic models assume that the asperities are flattened during contact. This is the same as assuming that the asperities penetrate into the smooth surface in the equivalent model, without any change in shape of the parts of the equivalent rough surface not yet in contact. Therefore, bringing two rough surfaces together within a distance Y is equivalent to removing the top of the asperities at a height Y above the mean plane. The assumption of pure plastic microcontacts enables the micromechanics to be specified completely by the mean slope m and the surfaces roughness σ, without having to assume some deterministic peak shapes, as with elastic microcontact models. Cooper et al.[7] derived the following relationships for contact of nominal flat rough surfaces, assuming plastically deformed hemispherical asperities whose height and surface slopes have Gaussian distributions, where the mean separation

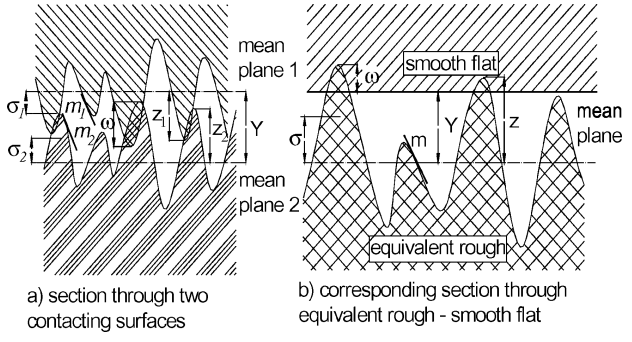

Fig. 1 Equivalent contact of conforming rough surfaces.

Y is constant throughout the contact plane:

$$a_s = \sqrt{8/\pi}\,(\sigma/m)\exp(\lambda^2)\operatorname{erfc}\lambda$$

$$n_s = \tfrac{1}{16}(m/\sigma)^2[\exp(-2\lambda^2)/\operatorname{erfc}\lambda]A_a$$

$$A_r/A_a = \tfrac{1}{2}\operatorname{erfc}\lambda \tag{2}$$

where $\lambda = Y/\sqrt{(2)}\sigma$, n_s, a_s, A_r, and A_a are the dimensionless mean plane separation, number and average size of microcontacts, and the real and the apparent contact area, respectively.

Microhardness

Microhardness is not constant throughout the material. Hegazy[8] demonstrated through experiments with four alloys that the effective microhardness is significantly greater than the bulk hardness. Microhardness decreases with increasing depth of the indenter until bulk hardness is obtained. He derived empirical correlations to account for the decrease in contact microhardness of the softer surface with increasing depth of penetration of asperities on the harder surface:

$$H_v = c_1(d_v')^{c_2} \tag{3}$$

where H_v is the Vickers microhardness in gigapascal, $d_v' = d_v/d_0$, $d_0 = 1$ μm, and c_1 and c_2 are correlation coefficients determined from the Vickers microhardness measurements.

Macrocontact Modeling

According to Johnson,[4] in static frictionless contact of solids, the contact stresses depend only on the relative profile of the two surfaces, that is, on the shape of the interstitial gap before loading. Hertz[1] replaced the two spheres contact geometry by a flat surface and a profile, which results in the same undeformed gap between the surfaces. Additionally, all elastic deformations can be considered to occur in one body, which has an effective elastic modulus E', and the other body is assumed to be rigid. The effective elastic modulus can be found from

$$1/E' = \left(1 - \upsilon_1^2\right)/E_1 + \left(1 - \upsilon_2^2\right)/E_2 \tag{4}$$

For the contact of two spheres, the effective radius of curvature is

$$1/\rho = 1/\rho_1 + 1/\rho_2 \tag{5}$$

As a result of the preceding assumptions and by considering axisymmetric loading, the complex geometry of two spherical rough surfaces is simplified to a rigid smooth sphere having the equivalent radius of curvature in contact with a rough flat, which has the equivalent surface characteristics (Fig. 2).

The open literature contains very few analytical mechanical models for the contact of spherical rough surfaces. The first in-depth analytical study to investigate the effect of roughness on the pressure distribution and deformation of contacting elastic spherical bodies was performed by Greenwood and Tripp.[9] Greenwood and Tripp developed their model based on the same assumptions as the Greenwood and Williamson[3] nominal flat rough contact model. Their assumptions can be summarized as follows:

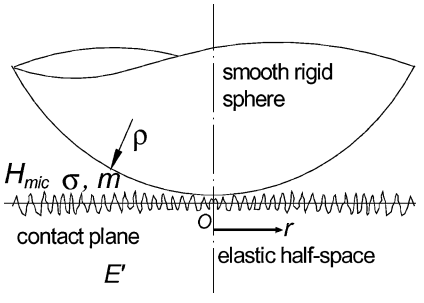

Fig. 2 Equivalent contact geometry of two spherical rough surfaces.

1) Contact is axisymmetric, and the bulk deformation is elastic.
2) Rough surfaces are isotropic with Gaussian height distribution and a standard deviation σ.
3) The distribution of summit heights is the same as the surface heights standard deviation, that is, $\sigma_s = \sigma$.
4) The deformation of each asperity is independent of its neighbors.
5) The asperity summits have a spherical shape, all with a constant radius β, the asperities entirely deform within the elastic limit, and Hertz[1] theory can be applied for each individual summit.

Greenwood and Tripp[9] derived a geometrical relationship relating the local separation to the bulk deformation and the sphere profile. The elastic deformations produced by a pressure distribution over an area of the surface can be calculated by superposition, using the Boussinesq solution for a concentrated load on a half-space, and the fact that the displacement due to an axisymmetric pressure distribution will also be axisymmetric. It can be shown that the normal displacement in a half-space due to an arbitrary pressure distribution can be found from[10]

$$\omega_b(r) = \begin{cases} \dfrac{2}{E'} \displaystyle\int_0^\infty P(s)\,\mathrm{d}s & r = 0 \\ \dfrac{4}{\pi E' r} \displaystyle\int_0^r s P(s) K\left(\dfrac{s}{r}\right) \mathrm{d}s & r > s \\ \dfrac{4}{\pi E'} \displaystyle\int_r^\infty P(s) K\left(\dfrac{r}{s}\right) \mathrm{d}s & r < s \end{cases} \tag{6}$$

where $\omega_b(r)$ is the local bulk deformation, $K(\cdot)$ is the complete elliptic integral of the first kind, and s is a dummy variable. Greenwood and Tripp[9] used Eq. (6), which gave a complementary relation between local separation and the pressure. They reported a complete set of relationships and solved it numerically.

The most important trends in the Greenwood and Tripp[9] model were that an increase in roughness resulted in a decrease in the contact pressure, compared with the Hertzian pressure, and that the effective macroscopic contact radius grew beyond the Hertzian contact radius. The Greenwood and Tripp[9] model is attractive for its mathematical simplicity, but it suffers from the following shortcomings:

1) A constant summit radius β is unrealistic. For a random surface, β is also a random variable.[11]
2) Two of its input parameters, that is, radius of summits β and density of summits η_s cannot be measured directly and must be estimated through statistical calculations. These parameters are sensitive to the surface measurements.[4]
3) Applying the model is complex and requires computer programming and numerically intensive solutions.
4) All asperities are assumed to deform elastically.

Tsukada and Anno[12] and Sasajima and Tsukada[13] with the same assumptions as Greenwood and Tripp[9] developed a model and offered expressions for pressure distribution as a function of nondimensional maximum pressure, $P_0/P_{0,H}$, and nondimensional radius of macrocontact area, a_L/a_H, for rough sphere–flat contacts. Tsukada and Anno[12] and Sasajima and Tsukada[13] presented these two parameters in a graphical form, in discrete curves, for relatively small radii of curvature, that is, 5, 10, and 15 mm and roughness in the range of 0.1–2 μm. They did not report general expressions for the maximum pressure and the radius of macrocontact.

Present Model

The micromechanical analysis of the present model is developed on the basis of the Cooper et al.[7] plastic model. The macrocontact area is divided into infinitesimal conforming surface elements where the conforming rough surface relationships, that is, Eqs. (2), can be applied. Bulk deformations are related to the local separation of the contacting surfaces, through a geometrical relationship similar to Greenwood and Tripp.[9] The assumptions of the present model can be summarized as follows:

1) Contacting surfaces are macroscopically spherical, which are considered as a sphere–flat contact (Fig. 2).
2) Microscopically, contacting surfaces are rough and isotropic with a Gaussian asperity distribution. Only one surface is taken to be rough, whereas the equivalent roughness is assumed to be on the flat plane and the sphere is assumed to be smooth.
3) Microcontacts deform plastically, and the asperity pressure is the local microhardness of the softer material in contact. Reasons supporting this assumption are discussed by Bahrami et al.[6]
4) Deformation of each asperity is independent of its neighbors.
5) Only the first loading cycle is considered.
6) The load is axisymmetric and the contact is frictionless, that is, there are no tangential forces in the contact area.
7) The macrocontact is elastic, where the elasticity theory given in Eq. (6) is employed to determine the substrate deformation.
8) The contact is static, that is, there is no relative motion or vibration effect.

In the vicinity of the contact region, the profile of the sphere can be written as

$$u(r) = u_0 - r^2/2\rho \tag{7}$$

Figure 3 shows the contact geometry after applying the load. The local separation $Y(r)$ is defined as the distance between two mean planes of the contacting surfaces and can be written as

$$Y(r) = \omega_b(r) - u(r) = \omega_b(r) - u_0 + r^2/2\rho \tag{8}$$

At each microcontact, a discrete point force is created as shown in Fig. 4. The sum of these discrete point forces must be equal to the external force F. It is assumed that the asperities of the rough surface behave like a plastic zone on an elastic half-space, in the sense that the effect of the discrete point forces on the elastic half-space is considered as an equivalent continuous pressure distribution $P(r)$. Note that all bulk deformations are assumed to occur in the elastic half-space, which has an effective elasticity modulus E', and the sphere is assumed to be rigid. Consider an infinitesimal surface

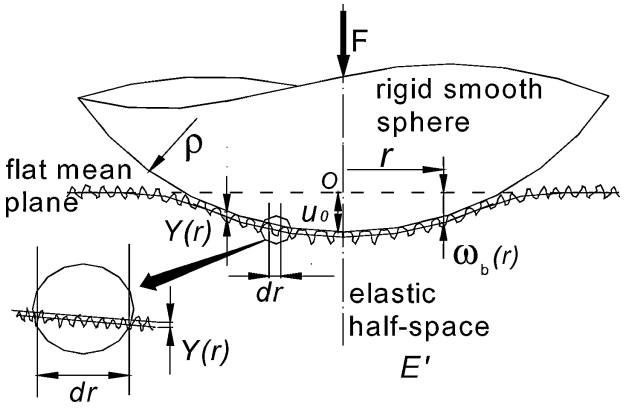

Fig. 3 Contact geometry after loading.

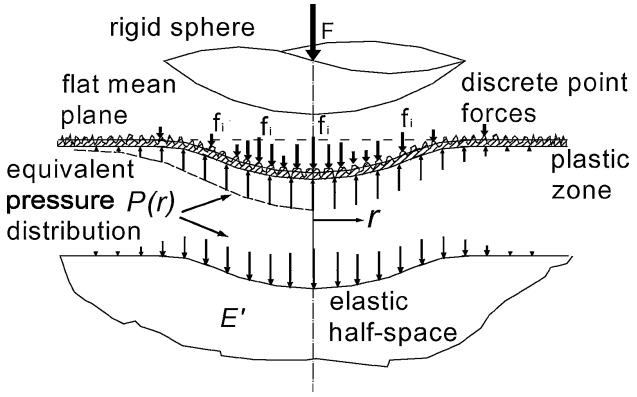

Fig. 4 Discrete point forces and the equivalent pressure distribution on the plastic zone.

element $dr \to 0$, where Fig. 3 shows a magnified element in which the local separation $Y(r)$ is uniform. The ratio of real to apparent area for a surface element can be found from Eq. (2),

$$dA_r(r)/dA_a(r) = \tfrac{1}{2}\operatorname{erfc}\lambda(r) \tag{9}$$

where $A_a(r) = 2\pi r\,dr$. As a result of surface curvature, the mean local separation and, consequently, the mean size of the microcontacts vary with radial position. The local microhardness can be determined from the Vickers microhardness correlation Eq. (3) as a function of the local mean microcontact radius. The relation between the Vickers diagonal d_v and the microcontact radius a_s, based on equal areas, is $d_v = \sqrt{(2\pi)}a_s$. Therefore, the local microhardness is

$$H_{\text{mic}}(r) = c_1\left[\sqrt{2\pi}\,a_s(r)\right]^{c_2} \tag{10}$$

where the local radius of the microcontacts can be found from Eq. (2)

$$a_s(r) = \sqrt{8/\pi}\,(\sigma/m)\exp[\lambda^2(r)]\operatorname{erfc}\lambda(r) \tag{11}$$

The external load F is the summation of the point forces at the microcontacts

$$F = \sum_i f_i = \iint_{\text{contact area}} A_r(r)H_{\text{mic}}(r) \tag{12}$$

When Eq. (9) is substituted into Eq. (12),

$$F = \pi\int_0^\infty H_{\text{mic}}(r)\operatorname{erfc}\lambda(r)\,r\,\mathrm{d}r \tag{13}$$

Instead of a_L, the upper limit of the integral is set to infinity because the macrocontact radius is not known and the effective pressure distribution rapidly approaches zero. On the bulk side, the equivalent pressure must satisfy the force balance,

$$F = 2\pi\int_0^\infty P(r)\,r\,\mathrm{d}r \tag{14}$$

The equivalent pressure distribution on the elastic half-space can be found from Eqs. (13) and (14),

$$P(r) = \tfrac{1}{2}H_{\text{mic}}(r)\operatorname{erfc}\lambda(r) \tag{15}$$

When the pressure distribution is known, the normal displacement of the bulk can be found from Eq. (6). Equations (6), (8), (10), (11), (14), and (15) form a closed set of governing relationships. A computer program was developed to solve the set numerically. The algorithm of the numerical solution is described in the Appendix.

No exact definition exists for the macrocontact radius in the literature. In this study, it is assumed to be the radius where the normalized pressure is negligible, that is, $P(r = a_L)/P_0 < 0.01$.

Numerical Results

A simulation procedure was run to construct the results shown in Figs. 5–8, based on the algorithms described in the Appendix and by using input data shown in Table 1. Contact of a stainless steel sphere-flat with an equivalent radius of curvature of 25 mm, equivalent surface roughness of 1.41 μm, and an applied load of 50 N was chosen as an example.

Figure 5 shows the pressure distribution predicted by the present model and the Hertzian pressure. It can be seen that due to the presence of roughness the maximum contact pressure compared to the Hertzian contact pressure is reduced and the load is spread over a greater area. The predicted macrocontact radius a_L is also shown in Fig. 5. Unlike the Hertzian pressure, the effective pressure falls asymptotically to zero. As expected, the mean radius of microcontacts a_s and microcontacts density η_s decrease as the radial position r increases. The microhardness profile is shown in Fig. 8.

To investigate the effect of roughness on the pressure distribution, the program was run for a wide range of roughness from 0.02 to 14.4 μm while all other parameters in Table 1 were kept constant. Figure 9 illustrates the effect of roughness on the pressure distribution. It can be seen that the effective pressure distribution approaches the Hertzian pressure distribution as the roughness decreases.

Table 1 Input parameters for a typical contact

Parameter	Value
ρ	25 mm
σ	1.41 μm
m	0.107
F	50 N
E'	112.1 GPa
c_1/c_2	6.27 GPa/−0.15

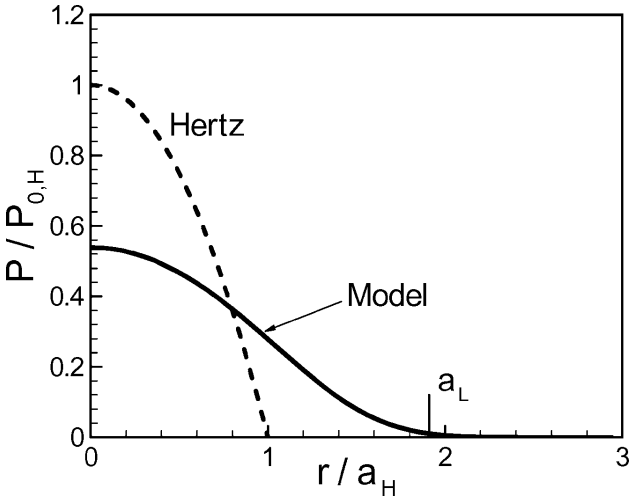

Fig. 5 Pressure distribution.

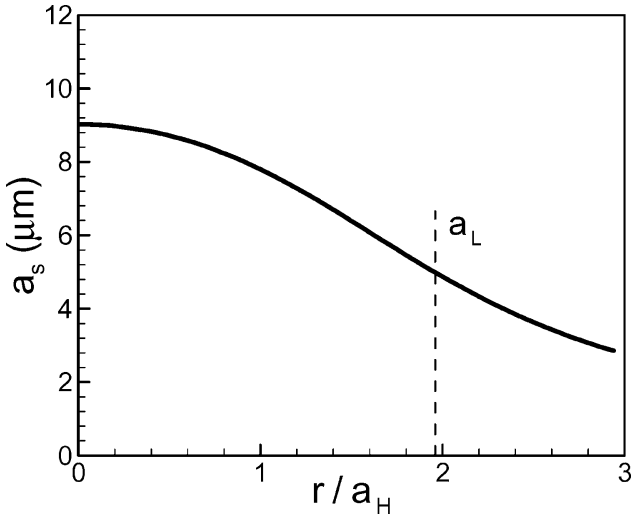

Fig. 6 Mean microcontacts radius.

Approximate Model

The main goal of this study is to develop simple correlations for determining the effective pressure distribution and the macrocontact radius as functions of nondimensional parameters that describe the contact problem. To develop an approximate solution, the following simplifications are made:

1) An effective microhardness H_{mic} that is constant throughout the contact region is considered.

2) The surface slope m is assumed to be a function of surface roughness, σ.

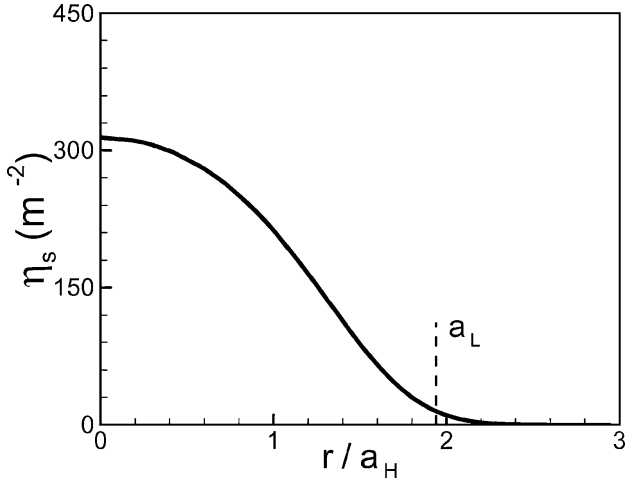

Fig. 7 Density of microcontacts.

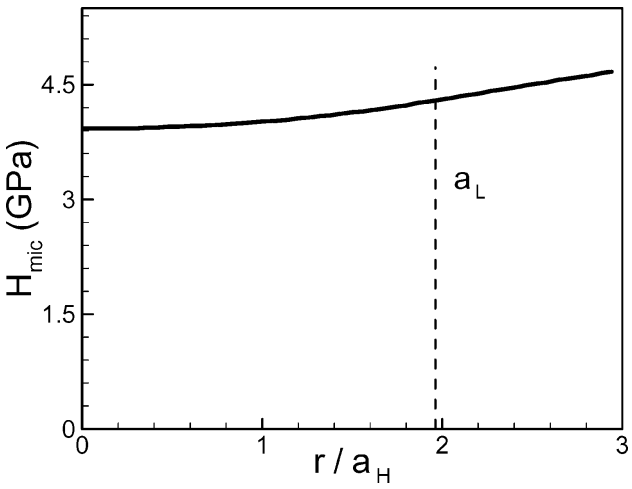

Fig. 8 Microhardness.

In this section, it is demonstrated that a general pressure distribution as a function of the maximum contact pressure exists. Then, with the use of dimensional analysis, the number of governing nondimensional parameters is determined, and finally, simple correlations for the maximum contact pressure and the macrocontact radius are proposed.

Figure 10 illustrates nondimensional pressure distributions for some values of $P_0' = P_0/P_{0,H}$ as function of nondimensional radial location $\xi = r/a_L$. It was observed that the nondimensional pressure distribution can be specified as a function of the dimensionless maximum pressure P_0' and the radial position ξ. In other words, a general profile exists that presents all possible pressure distributions.

The Hertzian pressure distribution[1] where the contacting surfaces are perfectly smooth is

$$P_H(r/a_H) = P_{0,H}\sqrt{1-(r/a_H)^2} \tag{16}$$

where

$$P_{0,H} = 3F\big/2\pi a_H^2, \qquad a_H = (3F\rho/4E')^{\frac{1}{3}}$$

The profile of the pressure distribution, especially in the contacts where the dimensionless maximum pressure is less than 0.6, is very similar to a normal (Gaussian) distribution. However, as the dimensionless maximum pressure approaches one (the Hertzian contact), the pressure distribution begins to deviate from the normal distribution profile. The general profile for the pressure distribution for spherical rough surface contact was found to be

$$P(\xi) = P_0(1-\xi^2)^{\gamma} \tag{17}$$

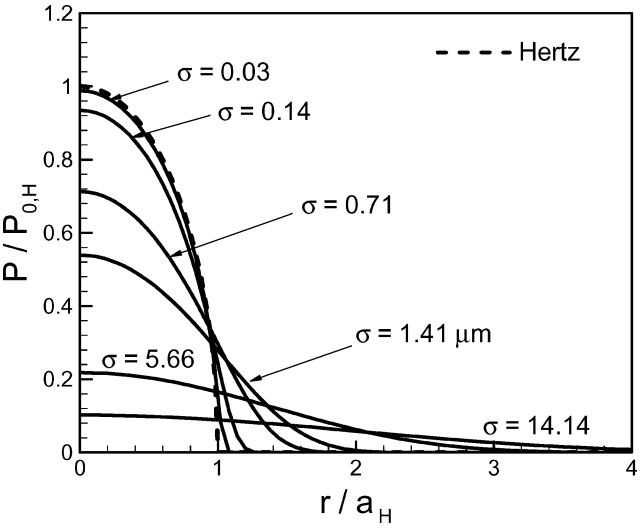

Fig. 9 Effect of roughness on equivalent pressure distribution.

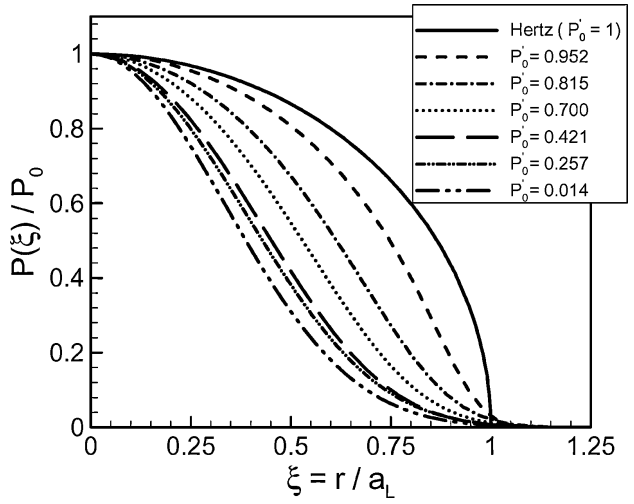

Fig. 10 Dimensionless pressure distributions for spherical rough surface contact.

where $\xi = r/a_L$ and γ can be calculated through a force balance

$$F = 2\pi \int_0^{a_L} P(r)\, r\, \mathrm{d}r \tag{18}$$

Substituting Eq. (17) into (18), after evaluating the integral, one finds

$$\gamma = 1.5P_0'(a_L')^2 - 1 \tag{19}$$

where $P_0' = P_0/P_{0,H}$ and $a_L' = a_L/a_H$.

At the limit, where roughness approaches zero, P_0' and a_L' both approach one, $\gamma = 0.5$, and Eq. (17) yields the Hertzian pressure distribution, Eq. (16). Knowing the general pressure distribution profile, that is, Eq. (17), the problem is reduced to finding relationships for P_0 and a_L. Additionally, the radius of the macrocontact area, based on its definition, can be found if P_0 and the pressure distribution are known; therefore, the key parameter is the maximum contact pressure P_0.

Dimensional Analysis

Dimensional analysis using the Buckingham Π theorem has been applied to many physical phenomena such as fluid flow, heat transfer, and stress and strain problems. The Buckingham Π theorem proves that in a physical problem including n quantities in which there are m dimensions the quantities can be arranged into $n-m$ independent

Table 2 Physical input parameters for spherical rough contacts

Parameter	Dimension
Effective elastic modulus E'	$ML^{-1}T^{-2}$
Force F	MLT^{-2}
Microhardness H_{mic}	$ML^{-1}T^{-2}$
Radius of curvature ρ	L
Roughness σ	L
Maximum contact pressure P_0	$ML^{-1}T^{-2}$

dimensionless parameters.[14] Table 2 summarizes the independent input parameters and their dimensions for spherical rough contacts. H_{mic} is an effective (mean) value for the microhardness of the softer material in contact.

Lambert and Fletcher,[15] using published experimental surface data, proposed a correlation for the absolute average asperity slopes, m, as a function of rms roughness σ,

$$m = 0.076\sigma^{0.52} \tag{20}$$

(See Bahrami et al.[6] for more detail.)

Because the surface slope m can be estimated using Eq. (20), it is not considered as an independent input parameter and is not included in Table 2.

All quantities in Table 2 are known to be essential to the maximum contact pressure, and hence, some functional relation must exist in the form of

$$P_0 = P_0(\rho, \sigma, E', F, H_{\text{mic}}) \tag{21}$$

When the Buckingham Π theorem is applied, there will be three Π groups so the maximum pressure can be more compactly stated as a function of these three nondimensional parameters. Johnson,[4] following the Greenwood and Tripp[9] model, introduced a nondimensional parameter α that we may call the roughness parameter, as the ratio of roughness over the Hertzian maximum bulk deformation, $\omega_{0,H}$

$$\alpha = \sigma/\omega_{0,H} \equiv \sigma\rho\Big/a_H^2 = \sigma(16\rho E'^2/9F^2)^{\frac{1}{3}} \tag{22}$$

The other nondimensional parameters were chosen to be τ, the geometric parameter, and E'/H_{mic}, the microhardness parameter. The geometric parameter τ is defined as

$$\tau = \rho/a_H = (4E'\rho^2/3F)^{\frac{1}{3}} \tag{23}$$

The computer program explained in the preceding section was run for a wide range of nondimensional (input) parameters, that is, $0.005 \le \alpha \le 100$ and $50 \le \tau \le 80{,}000$, to construct Figs. 11–14. These values of α and τ are chosen to span a wide range applicable to most thermal contact resistance problems. Values of α include the entire range of spherical rough contacts from very smooth (almost Hertzian $\alpha = 0$) to extremely rough contacts. The geometric parameter τ may be interpreted as a measure of the bulk strain. Because the bulk deformation is assumed elastic and also to justify the half-space assumption,[1] the radius of curvature must be much larger than the contact area, $\rho \gg a_H$. Thus, the lower bound of τ was fixed (arbitrarily) at $\tau = 50$, and the upper bound was selected to cover a relatively large radii of curvature and light loads.

The effect of microhardness parameter E'/H_{mic} on the maximum contact pressure P_0' was observed to be minimum and may be ignored (Figs. 11 and 12). Figure 13 shows the dimensionless maximum contact pressure in the form of a family of curves for a wide range of α and τ. As α decreases, which is equivalent to a decrease in roughness or an increase in radius of curvature or load, the dimensionless maximum pressure approaches 1 (the Hertzian pressure). Figure 14 shows the macrocontact radius as a function of α and τ. As can be seen, when α is decreased, the dimensionless radius of contact approaches one (the Hertzian contact). The dimensionless maximum contact pressure and the macrocontact radius plots were curve fitted. The following expressions can be used to estimate the

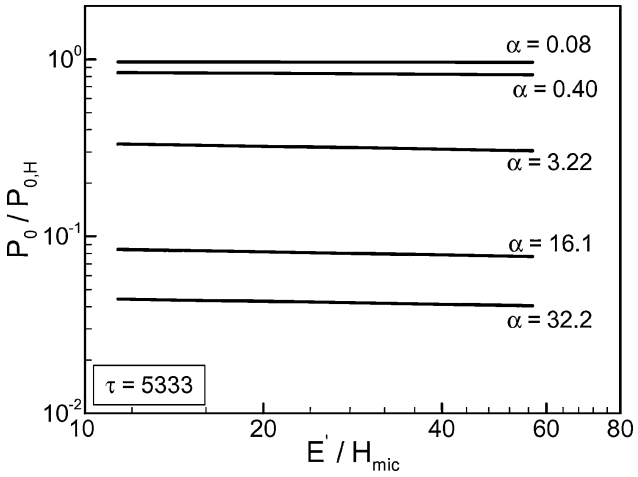

Fig. 11 Effect of microhardness on dimensionless maximum contact pressure, τ = 5333.

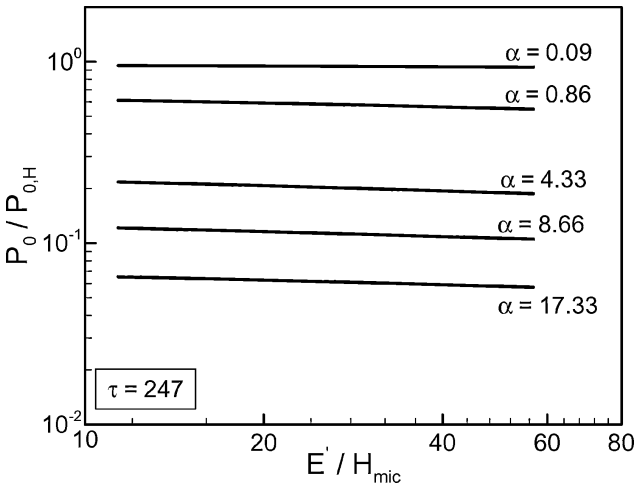

Fig. 12 Effect of microhardness on dimensionless maximum contact pressure, τ = 247.

maximum dimensionless contact pressure and the dimensionless radius of contact, respectively:

$$P_0' = P_0/P_{0,H} = 1\Big/\left(1 + 1.37\alpha\tau^{-0.075}\right) \tag{24}$$

$$a_L' = a_L/a_H = 1 - 1.50\,\ell_n P_0' - 0.14\,\ell_n^2\,P_0' - 0.11\,\ell_n^3\,P_0' \tag{25}$$

An expression for the nondimensional radius of the macrocontact, a_L', was developed as a function of α and τ in the form of $a_L' = c_0\sqrt{(\alpha + c_0')}$, where c_0 and c_0' are functions of τ only. In the limit where $\alpha \to 0$ (Hertzian contacts) as shown in Fig. 13, $a_L' \to 1$; therefore, a relationship between c_0 and c_0' can be found such that $c_0' = (1/c_0)^2$. Thus, c_0 was curve fitted, and the following correlation for a_L' was obtained

$$a_L' = \frac{a_L}{a_H} = 1.80\frac{\sqrt{\alpha + 0.31\tau^{0.056}}}{\tau^{0.028}} \tag{26}$$

The following approximate expression for a_L is proposed for contacts where the effective radius of curvature is relatively large, that is, approaching a flat surface

$$a_L' = 1.5\sqrt{\alpha + 0.45} \tag{27}$$

The rms difference between Eqs. (24–26) and the program results is estimated to be less than 8% in the range of $0 \le \alpha \le 100$ and $50 \le \tau \le 80{,}000$.

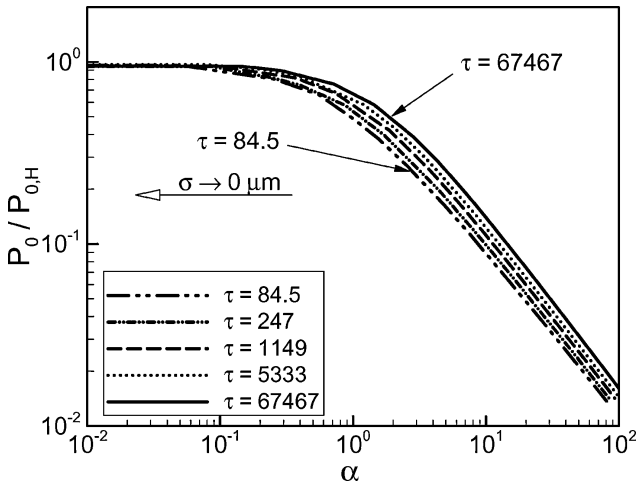

Fig. 13 Dimensionless maximum contact pressure.

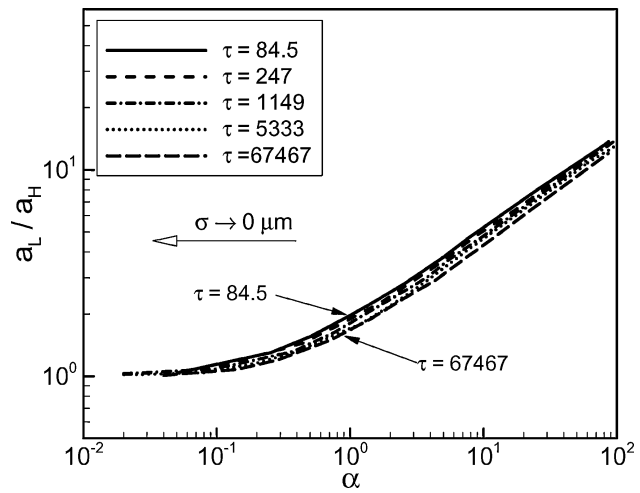

Fig. 14 Dimensionless radius of macrocontact.

Elastic Compression

In most engineering applications, the size of the contacting bodies is finite, and/or the radius of curvature is large, especially in the contacts where the surfaces are almost flat or slightly curved. When these surfaces are placed in contact, by applying a specific force that we call the critical force F_c, the macrocontact area reaches to the boundaries of the contacting bodies, that is, $a_L = b_L$, as shown in Fig. 15. When the force is increased beyond the critical force, the size of the macrocontact remains constant, but the contact pressure increases. Because the bulk deformation is assumed to be elastic, we refer to the preceding contact problems as elastic compression. Elastic compression cannot be treated as a half-space contact problem because the half-space assumption cannot be justified especially in the regions close to the edge of the contacting bodies. The critical force, the critical pressure distribution, and the pressure distribution associated with the critical force for a specified spherical rough contact assembly are unique.

In contact stress theory, the displacement at any point in the contact surface depends on the distribution of pressure throughout the whole contact. According to Johnson,[4] the earlier described interconnection may be avoided if the solids are modeled by a simple Winkler elastic foundation rather than a half-space. As shown in Fig. 16, the elastic compression approximation implies that as load passes the critical load the elastic foundation, which rests on a rigid base, is compressed by the rigid spherical indenter. There is no interaction between the springs of the model, that is, shear between adjacent elements of the foundation is ignored. Therefore, contact pressure at any point depends only on the displacement at that point. Equation (17) can be used to calculate the contact pressure distribution, where the external force is less than or equal to the critical load. Beyond the critical load, where $F > F_c$, the size of the macrocontact remains constant, and the elastic foundation approximation may be used to determine the pressure distribution. With assumption of the elastic foundation approximation, a uniform increase will be added to the critical pressure distribution at each point in the contact area. Therefore, the general pressure distribution can be summarized as

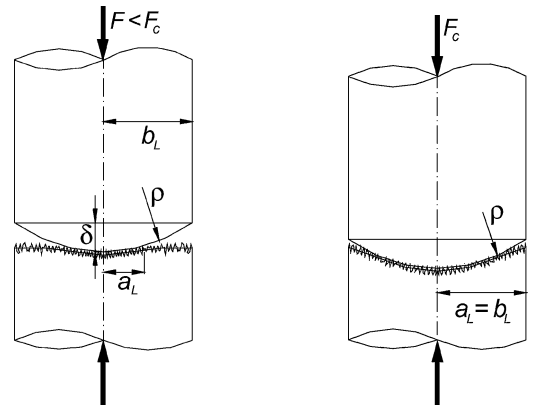

a) Half-space contact problem **b) Critical force**

Fig. 15 Contact of two finite spherical rough bodies.

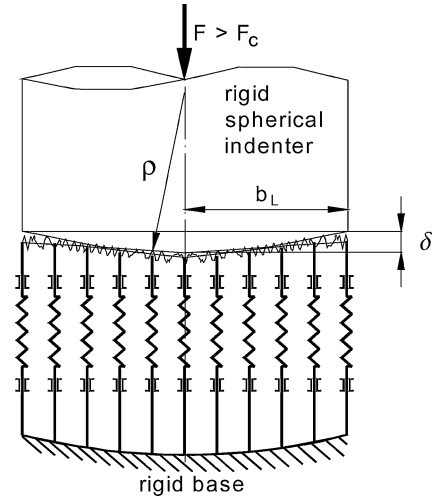

Fig. 16 Elastic foundation, Winkler model.

$$P(\xi) = \begin{cases} P_0(1-\xi^2)^{\gamma} & F \le F_c \\ P_{0,c}(1-\xi^2)^{\gamma_c} + (F - F_c)\big/\pi b_L^2 & F \ge F_c \end{cases} \quad (28)$$

where $a_L = b_L$ for $F \ge F_c$ and $P_{0,c}$ and γ_c are the maximum pressure and the exponent of the critical pressure distribution, respectively. Figure 17 shows the predicted pressure distributions for some values of the external load as an example. The parameters of the contact are $\rho = 10$ m, $E' = 112$ GPa, $\sigma = 2$ μm, and $b_L = 12$ mm.

To find a relationship for the critical force, Eqs. (24) and (27) should be solved simultaneously where $a_L = b_L$. Equation (27) is a function of α only, and it was developed for relatively large radii of curvature, that is, the situations where the elastic compression more likely occurs. The critical force can be estimated from

$$F_c = (4E'/3\rho)\Big[\max\Big\{0, \big(b_L^2 - 2.25\sigma\rho\big)\Big\}\Big]^{\frac{3}{2}} \quad (29)$$

where $\max\{x, y\}$ returns the maximum value between x and y.

A criterion for defining the flat surface where the surface curvature has a negligible effect on the pressure distribution can be derived by setting $F_c = 0$. Setting $F_c = 0$ means that if no load is applied $a_L = b_L$; thus, the contacting surfaces are ideally flat, which leads to

$$b_L^2\big/\sigma\rho \le 2.25 \quad (30)$$

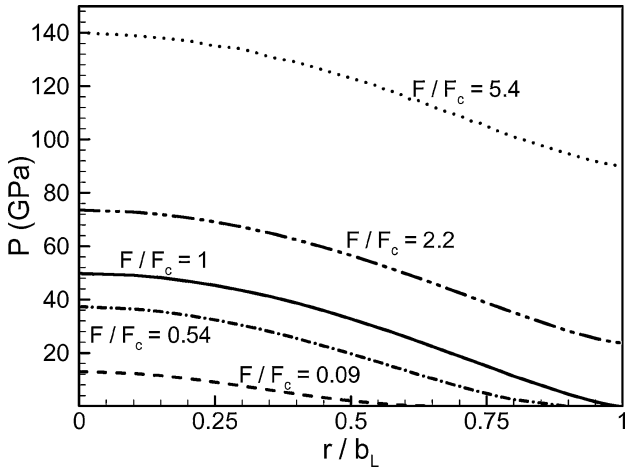

Fig. 17 Contact pressure distribution.

For spherical surfaces with large radii of curvature, Clausing and Chao[16] used a geometrical approximation that relates the maximum out-of-flatness δ (Fig. 16) to the radius of curvature,

$$\rho = b_L^2 \big/ 2\delta \tag{31}$$

When Eqs. (30) and (31) are combined, the flat surface criterion in terms of surface out-of-flatness can be obtained as

$$\delta/\sigma \leq 1.12 \tag{32}$$

In other words, if the out-of-flatness and the roughness of a surface are in the same order of magnitude, the surface is flat, that is, surface curvature has no effect on the contact pressure distribution. This criterion is derived based on the concept that the effect of surface curvature on the contact pressure is negligible in flat or conforming contacts. In the second part of this study,[17] another criterion will be defined based on a thermal contact resistance prespective.

Conclusions

The mechanical contact of spherical rough surfaces was studied, and a new analytical model was developed. The deformations of surface asperities were considered to be plastic, and the bulk deformation was assumed to remain within the elastic limit.

A closed set of governing relationships was derived and solved numerically. A computer code was developed to solve the governing relationships. The algorithm of the numerical procedure is explained in the Appendix. The pressure distributions predicted by the model were plotted for different values of surface roughness, and it was shown that as the surface roughness approaches zero the predicted pressure distribution approaches the Hertzian pressure.

Additionally, it was shown that a general pressure distribution profile exists that encompasses all spherical rough contacts. The maximum contact pressure was observed to be the key parameter that specifies the contact pressure distribution. The suggested general pressure distribution expression yields the Hertzian contact pressure at the limit, where roughness is set to zero.

When dimensional analysis was used, the number of independent nondimensional parameters that describe the maximum contact pressure was determined to be three, the roughness α, the geometric τ, and the microhardness E'/H_{mic} parameters. The effect of the microhardness parameter E'/H_{mic} on the maximum contact pressure was observed to be small and ignored. When curve-fitting techniques were used, simple correlations were suggested for calculating the maximum contact pressure distribution and the radius of the macrocontact area, as functions of roughness α, and geometric parameters τ.

An expression for estimating the critical load was derived, where $a_L = b_L$. The Winkler approximation was used to derive a relationship for the contact pressure distributions, where the loads are higher than the critical load. This expression along with the described correlation formed a general pressure distribution that encompasses all possible contact cases ranging from the smooth Hertzian to the conforming rough contact.

Also a criterion was offered to identify the flat surface, where the effect of surface curvature on the contact pressure can be neglected. Based on this criterion, the surface can be considered flat if the surface out-of-flatness and roughness are in the same order of magnitude.

The advantages of the present model over the Greenwood and Tripp[9] (GT) model are as follows:

1) The present model requires two input surface parameters, roughness σ and surface slope m. The GT model needs three input parameters, that is, σ, β, and η.

2) Unlike the summit radius β and the microcontact density η in the GT model, the present model input parameters can be measured directly, and they are not sensitive to the surface measurements.

3) A pressure distribution profile was proposed as a function of the maximum contact pressure, which covers all possible contact cases.

4) Simple correlations for determining the maximum contact pressure and the radius of macrocontact as functions of two nondimensional parameters, that is, the roughness parameter α and the geometric parameter τ, were offered.

Appendix: Numerical Procedure

The following procedure (Fig. A1) is used to solve the governing set of relationships outlined in the present model. A value of $u_{0,1}$ is assumed, and pressure distribution is computed. $P(r)$ is then used to calculate an improved ω_b (r). This improved ω_b (r) now is used to calculate a new pressure distribution P_{new} (r), and so on, until P (r) converges. The algorithm of the preceding procedure is shown in the inner loop flow chart, Fig. A2. The pressure distribution P (r) is integrated and compared with the external load F, and the relative force error F_1^* is calculated. Here $u_{0,2}$ is assumed, and all of the mentioned steps are repeated for $u_{0,2}$ to compute F_2^*. With the use of linear interpolation, u_{new} and then F_{new}^* are similarly

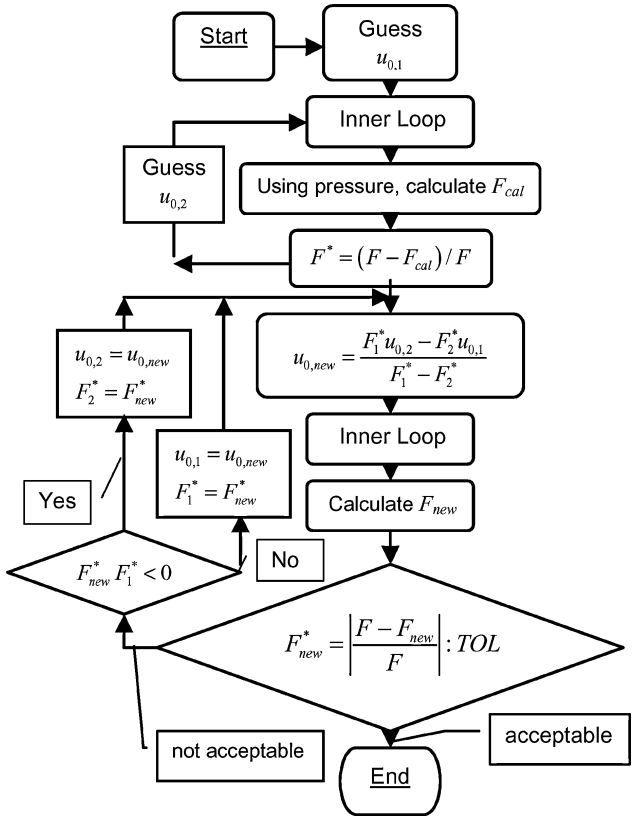

Fig. A1 Numerical algorithm.

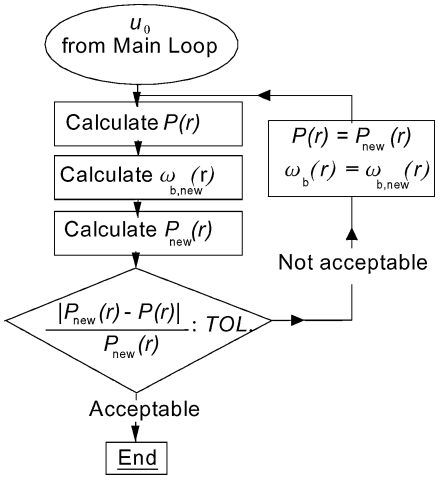

Fig. A2 Pressure-displacement iteration procedure, the inner loop.

calculated by using the inner-loop procedure. If F^*_{new} is not within the acceptable tolerance, u_0 and F^* are updated, and the iterative pressure–displacement calculation procedure is repeated until the convergence is achieved. The loop is continued until the integrated pressure and external load are within an acceptable tolerance.

References

[1]Hertz, H., "On the Contact of Elastic Bodies," *Journal fur die reine und angewandie Mathematic*, Vol. 92, 1881, pp. 156–171 (*in German*).

[2]Tabor, D., *The Hardness of Metals*, Oxford Univ. Press, Amen House, London, 1951.

[3]Greenwood, J. A., and Williamson, B. P., "Contact of Nominally Flat Surfaces," *Proceedings of the Royal Society of London, Series A: Mathematical and Physical Sciences*, Vol. A295, 1966, pp. 300–319.

[4]Johnson, K. L., *Contact Mechanics*, Cambridge Univ. Press, Cambridge, England, U.K., 1985.

[5]Williamson, J. B., Pullen, J., Hunt, R. T., and Leonard, D., "The Shape of Solid Surfaces," *Surface Mechanics*, American Society of Mechanical Engineers, New York, 1969, pp. 24–35.

[6]Bahrami, M., Culham, J. R., Yovanovich, M. M., and Schneider, G. E., "Review of Thermal Joint Resistance Models for Non-Conforming Rough Surfaces in a Vacuum," American Society of Mechanical Engineers, Paper HT2003-47051, July 2003.

[7]Cooper, M. G., Mikic, B. B., and Yovanovich, M. M., "Thermal Contact Conductance," *International Journal of Heat and Mass Transfer*, Vol. 12, 1969, pp. 279–300.

[8]Hegazy, A. A., "Thermal Joint Conductance of Conforming Rough Surfaces: Effect of Surface Micro-Hardness Variation," Ph.D. Dissertation, Dept. of Mechanical Engineering, Univ. of Waterloo, Waterloo, ON, Canada, 1985.

[9]Greenwood, J. A., and Tripp, J. H., "The Elastic Contact of Rough Spheres," *Journal of Applied Mechanics*, Vol. 89, No. 1, 1967, pp. 153–159.

[10]Gladwell, G. M. L., *Contact Problems in the Classical Theory of Elasticity*, Sijthoff and Noordhoff, Alphen aan den Rijn, The Netherlands, 1980, pp. 81–86.

[11]Francis, H. A., "Application of Spherical Indentation Mechanics To Reversible and Irreversible Contact Between Rough Surfaces," *Wear*, Vol. 45, 1977, pp. 221–269.

[12]Tsukada, T., and Anno, Y., "On the Approach Between a Sphere and a Rough Surface, 1st Report—Analysis of Contact Radius and Interface Pressure," *Journal of the Japanese Society of Precision Engineering*, Vol. 45, No. 4, 1979, pp. 473–479 (*in Japanese*).

[13]Sasajima, K., and Tsukada, T., "On the Approach Between a Sphere and a Rough Surface, 2nd Report—Critical Condition to Yield Plastic Deformation in Contacting Bodies," *Journal of the Japanese Society of Precision Engineering*, Vol. 47, No. 6, 1981, pp. 694–699 (*in Japanese*).

[14]Streeter, V. L., and Wylie, E. B., *Fluid Mechanics*, McGraw–Hill, New York, 1975, Chap. 4.

[15]Lambert, M. A., and Fletcher, L. S., "Thermal Contact Conductance of Spherical Rough Metals," *Transactions of ASME: Journal of Heat Transfer*, Vol. 119, No. 4, 1997, pp. 684–690.

[16]Clausing, A. M., and Chao, B. T., "Thermal Contact Resistance in a Vacuum Environment," *Journal of Heat Transfer*, Vol. 87, 1965, pp. 243–251; also ASME Paper 64-HT-16, 1964.

[17]Bahrami, M., Culham, J. R., Yovanovich, M. M., and Schneider, G. E., "Thermal Contact Resistance of Non-Conforming Rough Surfaces Part 2: Thermal Model," *Journal of Thermophysics and Heat Transfer*, Vol. 18, No. 2, 2004, pp. 218–227; also AIAA Paper 2003-4198, June 2003.